ISSN 2310-4090

International Journal of Scientific Footprints Open Access

Investigations on Geo-effective parameters of Halo Coronal Mass Ejections

A. Mujiber Rahman[1], S. Umapathy[2], V. Vasanth[3]

[1]Department of Physics, Hajee Karutha Rowther Howdia College, Uthamapalayam – 625 533, India.
[2]School of Physics, Madurai Kamaraj University, Madurai- 625 021, India.
[3] Department of Physics, Shangdong University, China.

Keywords:
Sun- Coronal Mass Ejections-type II; bursts-geomagnetic storms.

Correspondence:
A. Mujiber Rahman, Department of Physics, Hajee Karutha Rowther Howdia College, Uthamapalayam – 625 533, India
E-mail: mujib73@gmail.com

Funding Information:
No funding information provided.

Received:
October 2014; Accepted: November 2014

International Journal of Scientific Footprints 2014; 2(5): 34–47

Abstract

We have examined the physical characteristics of 67 halo coronal mass ejections (CMEs) and their geo-effective parameters during the year 2012. By examining all SOHO EIT and SOHO LASCO images of the CMEs, 67 halo CMEs are selected and examined their association with solar activities such X-ray flares and type II bursts. Further, we examined the geomagnetic effects of these entire halo CMEs at 1 AU. We found that 70% of CME events associated with X-ray flares. Out of 67 events, only 9 events associated with type II bursts. It is also found that majority of the type II bursts associated with faster CMEs (>1300 km/s). In particular, the CME direction parameter, which is defined as the maximum ratio of its shorter front from solar disk center and its longer one, is proposed as a new geo-effective parameter (Moon et al., 2005). Its major advantage is that it can be directly estimated from coronagraph observation. It is found that while the location of the associated flare has a poor correlation with the Dst index, the new direction parameter has a relatively good correlation.

Introduction

It is established that Coronal Mass Ejections (CMEs) are thought to be geo-effective objects producing geomagnetic storms at 1 AU during the past several decades. Several authors (Moon et al., 2002, Sheeley et al., 1999, Andrews & Howard, 2001) suggested that flare associated CMEs shows higher speeds and low accelerations, whereas eruptive filament associated CMEs shows lower CME speeds and large accelerations.

By analysing both the front and back side halo CMEs to determine the geo-effectiveness of the very fast CMEs, we select halo CMEs observed by SOHO LASCO during the solar maximum year of Solar Cycle 24. We also observed that many front sided halo CMEs produce geomagnetic storms, since they are thought to be good potential candidates that can produce strong geomagnetic storms (e.g.,Wang et al. 2002; Zhang et al. 2003; Zhao &Webb 2003). Also, we noted that not all front sided CMEs are Geo-effective as suggested by St. Cyr et al., (2000). Cane et al. (2000) showed that only about half of front-side halo CMEs encountered the Earth, and their associated solar events typically occurred from 40° east to 40° west in longitude. Mujiber Rahman et al. (2010) analyzed Geo-effectiveness of 91 disc centered (± 30°) CME events and found that only 40% of the events produced moderate (Dst ≤ -75 nT) to severe (Dst ≤ - 200 nT) geomagnetic storms. But all these 91 CMEs are not only halo CMEs, the list includes partial halo CMEs also. Moon et al. (2005) found the Geo-effectiveness of 12 front sided halo CMEs and it is well known that a significant fraction of halo CMEs are Geo-effective. According to previous studies (Cane et al. 2000; Wang et al. 2002, Moon et al. 2005, Gopalswamy et al. 2009), only about 50% of all halo CMEs are Geo-effective, and the others are not. In addition, most of the Geo-effective halo CMEs originated near the central meridian of the Sun when the locations of their associated flares are used. Thus, we may suppose that halo CMEs that originated near the central meridian have higher possibilities of causing strong geomagnetic storms.

2. Data Selection

In the present study, we have analyzed 67 Halo CME events as listed in SOHO LASCO website http://www.cdaw.gsfc.nasa.gov. The LASCO C2 instrument is an externally occulted white light coronagraph that observes Thomson-scattered visible light through a broadband filter. It covers 2–6 $R_\odot$ with a pixel resolution of 12”.1 (Brueckner et al. 1995). We consider the SOHO LASCO CMEs classified as Halo CMEs whose speeds are in the range ~500 km/s to ~1800 km/s from the SOHO LASCO online catalog. Also we inspected all EIT and LASCO images of these events and their running difference images, to identify whether they are front-sided events and whether the CMEs are associated with flares. The flare data is obtained from online catalog using the website ftp://ftp.sec.noaa.gov/. We also examined the associations of these CMEs with interplanetary type II radio bursts whose information is archived by http://ssed.gsfc.nasa.gov/waves. Geomagnetic storm index (Dst) values were found for all the 67 Halo CME events with a time window of 2 to 3 days from CME date from the available online catalog http://swdcwww.kugi.kyoto-u.ac.jp/dstdir/index.html. The list of all the 67 Halo CMEs and their associated flare and radio bursts are found in Table 1. Month, date and time of all the CMEs obtained are listed in column 1 – 3 in Table 1. Acceleration, Width and Speed of all the CMEs are listed in column 4 – 6 in Table 1. The corresponding geomagnetic storm date, time and strength of the storm of all the 67 events are listed in column 7 – 9 in Table 1. The direction parameter calculated for the all the events are listed in column 10 of Table 1. Radio bursts and X ray flares associated with all the CMEs are listed in columns 11 and 12, respectively.

3. Results and Discussion

Figure 1. Distribution diagram of CME Speeds and the number of events

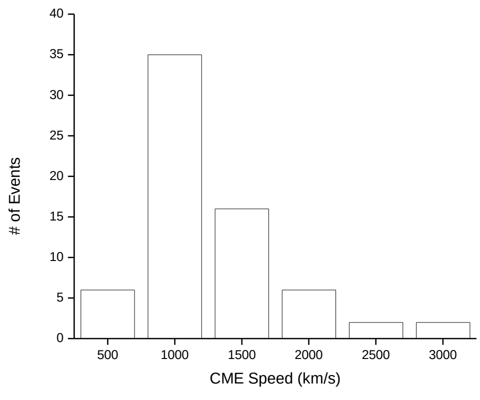

Fig. 1 shows the distribution diagram of CME speeds, we noted that the speed of the Halo CMEs is uniformly distributed and a large number of events are in the speed range of ~1000 km/s. We found that 35 events out of 67 events are observed in the speed range of ~1000 km/s and 16 events are found in the speed range of ~1500 km/s. It is also noted that very high speed (~3000 km/s) and very low speed (~500 km/s) CMEs are very less in number.

Figure 2. Distribution of acceleration of CME with number of events

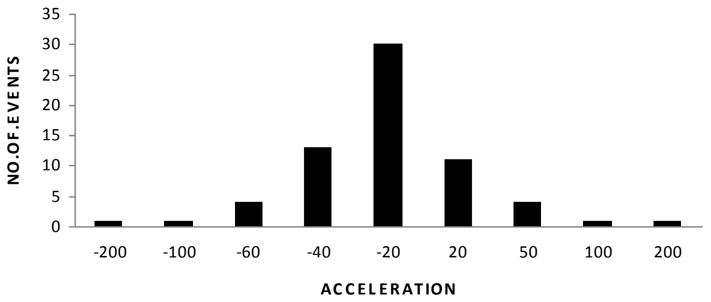

From Fig. 2, we found that large number of events shows negative acceleration than the positive acceleration. This may be due to the fact that fast CMEs are decelerating and slow CMEs are accelerating while initiating as observed from the SOHO LASCO site (see, e.g., Manoharan and Mujiber Rahman, 2011, Mujiber Rahman et al., 2013). As the large number of Halo CMEs observed in the solar maximum year corresponds to the speed of ~1000 to ~1500 km/s and these CMEs are suffering deceleration is well observed from the Fig. 2. Manoharan (2006), confirmed that the accelerations as well as decelerations of CMEs are due to the exchange of energy between the CME and solar wind. From Fig. 1 we observed that some 35 CMEs are associated with the speed of 1000 km/s and they shows the acceleration in the range of -20 m/sec^2 and the very fast CMEs shows the acceleration range -200 m/sec^2 and -100 m/sec^2, respectively. Also, we noted that the 5 slow speed CMEs in the positive acceleration in the range of 50 to 100 m/sec^2.

Figure 3: Distribution diagram of Transit time with the number of events

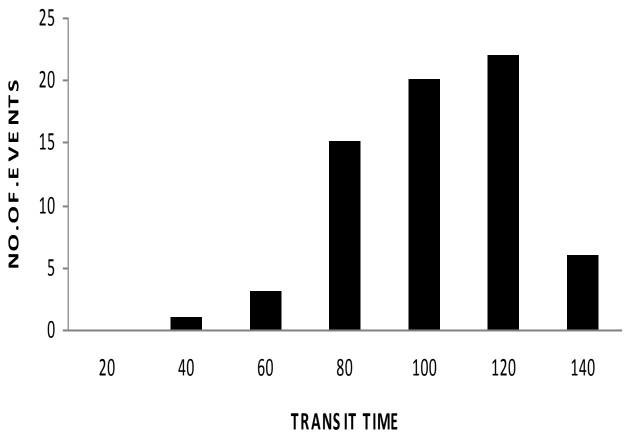

Fig. 3, shows the distribution diagram of transit time with the total number of Halo CME events. The travel time of a CME to the Earth is an indicator of its typical average speed between LASCO FOV and the Earth (see, e.g., Manoharan and Mujiber Rahman, 2011). From this figure, we observed that a large number of events show travel time in the range of 80 to 120 hours. Very few numbers of events are observed in the transit time range of 40 to 60 hours. The events with lower transit time are corresponding to higher CME speed events and we note that events with low CME speed are corresponding to the higher transit time. So that, we can concluded that higher speed CME events with lower transit time to 1 AU and vice versa. This result is in consistent with Mujiber Rahman, et al., (2013).

Here we note that the location parameter may not properly indicate the central axis of the Interplanetary Coronal Mass Ejection's propagation direction at least in some cases. As a more direct parameter, Moon et al., (2005) proposed a direction parameter that can be directly available from coronagraph observations. In our present study, let us consider the shape of two halo CMEs, as shown in Fig. 4. If the front of a CME is directly propagating toward the Earth, the shape in its pre-event subtracted image should be nearly symmetric (like a circle) as shown in the left panel of Fig. 4. If the front of a CME is propagating away from the Sun-Earth line, its shape should be quite asymmetric, as seen in the right panel of Fig. 1.

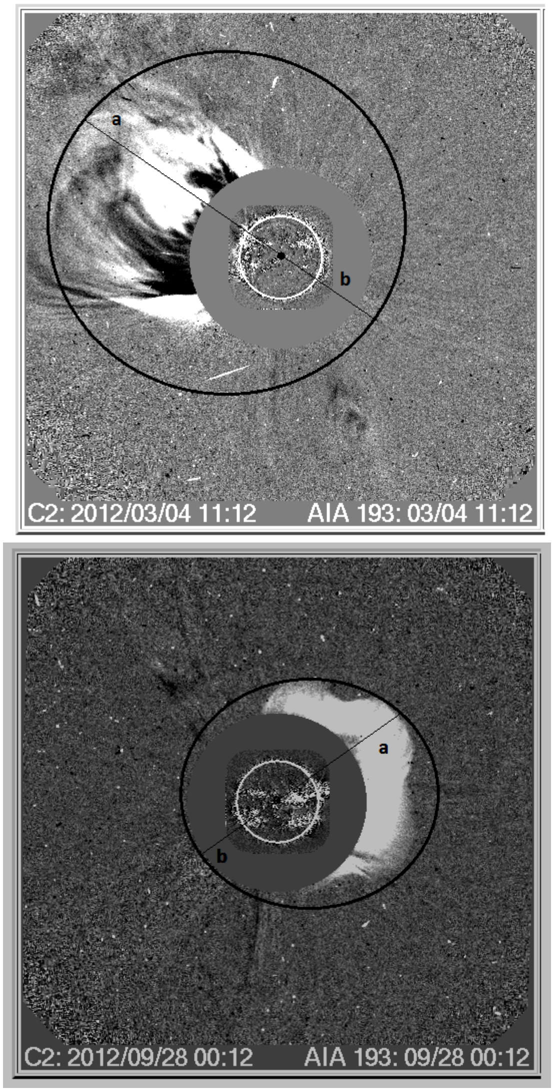

Figure 4. LASCO C2 running difference images of the 2012 March 04 event (left) and the 2012 September 28 event (right). How to estimate a and b is described in text

To quantify its symmetric characteristics, Moon et al. (2005) suggested a quantitative parameter as follows: (1) a pre-event image is subtracted, (2) an ellipse is plotted on the image and then its major and minor axes are manually adjusted in such a way that the ellipse can approximately follow the front edge of a CME, (3) straight lines connecting pairs of opposite positions on the CME front are considered, (4) the ratio (b/a) between the shorter distance (b) from the solar disk center and the longer distance (a) is obtained, and (5) its maximum value is finally estimated as the direction parameter; equivalently, the line having the maximum ratio corresponds to an extension of the line connecting solar center and the center of the ellipse. Geometrically, the proposed parameter depends on the ratio of the distance between the ellipse center and solar center to the distance between the center of the ellipse and the CME front. While the direction parameter (DP = b/a) of the 2012 March 04 event (left) of Figure 4 is 0.48, the parameter of the 2012 September 28 event (right) is 0.64. This fact implies that the second event is more symmetric than the first one; that is, the direction of the second event is more oriented toward the Earth. In fact, while the second CME is associated with a very strong geomagnetic storm (Dst = -131 nT), the first CME did not produce any remarkable geomagnetic activity.

Figure 5. CME speed observed in SOHO LASCO is correlated with disturbance storm time (Dst) index values.

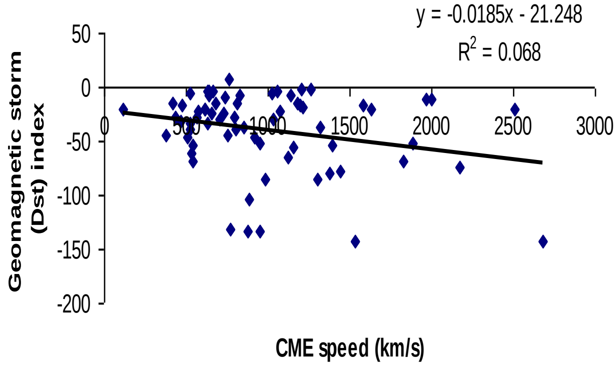

We correlated the CME speeds 67 Halo events which is observed using the SOHO LASCO CME list with geomagnetic storm index (Dst) values found using the Kyoto website. We noted from the Fig. 5, the two values are not correlated well with a correlation coefficient of r = 0.26. Also, we noted that slow speed CME events are not capable of producing strong geomagnetic storms. We observed from our list of events is that the events with CME speed > 900 km/s only producing strong geomagnetic storms.

Figure 7. Correlation of CME direction parameter Vs geomagnetic storm index values

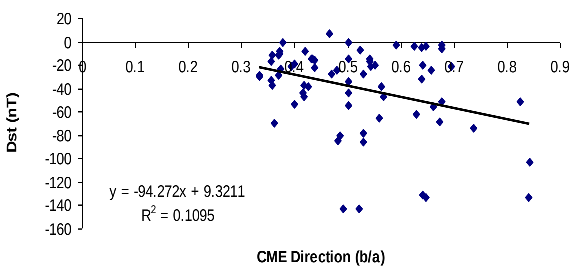

Moon et al., (2005) introduced the direction parameter is proposed as a new geo-effective parameter. Its main advantage is that it can be directly estimated from coronagraph observation, as well as that it is well understood as a geometrical concept. In Fig. 6, we correlated the direction parameter (b/a) values of 67 Halo CMEs with their corresponding geomagnetic storm index (nT) values. We noted that lower direction parameter values shows low geomagnetic storms, but higher (b/a) values shows strong geomagnetic storm values. This result is in consistent with Moon et al., (2005) and Kim et al., (2008).

Conclusions

In the present work, we analyzed 67 Halo CME events observed by SOHO LASCO field of view in the solar maximum year. The speed range of these events is ~500 km/s to 1800 km/s. The acceleration values of all these events are found in the SOHO/LASCO field of view. The acceleration values are in the range ~ -159 m/s^2 to 165 m/ s^2. From the earlier studies, we understand that higher CME speed events are decelerating while the slower CME speeds are accelerating due to the propagation of CMEs are affected by the solar wind. That is, there is an exchange of energy between the CME and the solar wind.

As we have observed from the Fig. 1, most of the halo CMEs observed in the speed range of ~1000 to ~1500 km/s. Very high speed and very low speed CMEs are very less in number. From the Fig. 2, we noted that as the large number of Halo CMEs observed in the solar maximum year corresponds to the speed of ~1000 to ~1500 km/s, these CMEs are suffering deceleration is well observed from the above figure. The accelerations as well as decelerations of all the CMEs are due to the exchange of energy between the CME and solar wind.

The travel time of a CME to the Earth is an indicator of its typical average speed between LASCO FOV and the Earth (see, e.g., Manoharan and Mujiber Rahman, 2011). From the Fig. 3, we observe that a large number of events have travel time in the range 80-120 hours. Very few numbers of events are observed in the transit time range of 40- 60 hours. Further, Moon et al., (2005) proposed a new direction parameter that can be directly available from coronagraph observations (refer Fig. 4). While the direction parameter (b/a) of the 2012 March 04 event (left) of Fig. 4 is 0.48, the parameter of the 2012 September 28 event (right) is 0.64. This fact implies that the second event is more symmetric than the first one; that is, the direction of the second event is more oriented toward the Earth. In fact, while the second CME is associated with a very strong geomagnetic storm (Dst= -131 nT), the first CME did not produce any remarkable geomagnetic activity.

We correlated the CME speeds 68 Halo events which is observed using the SOHO LASCO CME list with geomagnetic storm index (Dst) values found using the Kyoto website. We noted from the Fig. 5, the two values are well correlated with a correlation coefficient of r = 0.068. Also, we noted that slow speed CME events are not producing strong geomagnetic storms. In Fig. 6, we correlated the direction parameter (b/a) values with geomagnetic storm index (nT) values and we noted that lower direction parameter values shows low geomagnetic storms, but higher b/a values shows strong geomagnetic storm values. This is in consistent with Moon et al., (2005). Kim et al. (2008), showed that most of the geo-effective events with direction parameter value is greater than 0.4. From the correlation plots we found that, when (b/a) value is increases the Dst values also found to increases.

References

[1] Blackman, Eric G.; Brandenburg, Axel, 2003, Doubly Helical Coronal Ejections from Dynamos and Their Role in Sustaining the Solar Cycle, ApJ, 584, L99-L102.

[2] Brueckner, G.E., Howard, R.A., Koomen, M.J., Korendyke, C.M., Michels, D.J., Moses, J.D., Socker, D.G, & Linker, J. 1995, TheLarge Angle Spectroscopic Coronagraph (LASCO) Sol. Phys., 162, 357.

[3] Gopalswamy, N., Lara, A., Lepping, R.P., Kaiser, M.L., Berdichevsky, D., St. Cyr, O.C.: 2000. Geophys. Res. Lett. 27, 145.

[4] Gopalswamy, N., Lara, A., Manoharan, P.K., Howard, R.A.: 2005. Adv. Space Res. 36, 2289.

[5] Manoharan, P.K.: 2006. Solar Phys. 235, 345.

[6] Manoharan, P.K., Mujiber Rahman, A. Coronal mass ejections propagation time and associated internal energy. J. Atmos. Sol. Terr. Phys. 73, 671–677, 2011.

[7] Mujiber Rahman, A., Umapathy, S., Shanmugaraju, A., Moon, Y.J. 2012. Solar and interplanetary parameters of CMEs with and without type II radio bursts. Adv. Space Res. 50, 516–525.

[8] Mujiber Rahman, A., Shanmugaraju, A., Umapathy, S. 2013. Propagation of normal and faster CMEs in the interplanetary medium, Adv. Space Res. 52, 1168-1177.

[9] Moon, Y. –J., Cho, K. –S., Dryer, M., Kim, Y. –H., Bong, S. –C., Chae, J., Park, Y.D., 2005, New Geo-effective parameters of very fast Halo Coronal Mass Ejections, ApJ, 624, 414.

[10] Parker, E.N.: 1958. Physics of Fluids. 1, 171.

[11] Kim, R. –S., Cho, K. –S., Kim, Y. –H., Park, Y.D., Moon, Y. –J., Yi, Y, Lee, J., Wang, H., Song, H., 2008, CME Earthward direction as an important Geo-effectiveness indicator, ApJ, 677, 1378.

[12] Klimchuk, J. A., 2001, Theory of Coronal Mass Ejections, Space Weather (Geophysical Monograph 125), ed. P. Song, H. Singer, G. Siscoe (Washington: Am. Geophys. Un.), 143.

[13] Kopp, R. A.; Pneuman, G. W., 1976, Magnetic reconnection in the

corona and the loop prominence phenomenon, Solar Physics, 50, 85-98.

[14] Low, B. C.; Fong, B.; Fan, Y., 2003, The Mass of a Solar Quiescent Prominence, ApJ, 594, 1060-1067.

[15] Low, B. C., 1996, Solar Activity and the Corona, Solar Physics, 167, 217-265.

[16] Low, B. C., 1999, Coronal Mass Ejections, flares and prominences, he solar wind nine conference. AIP Conference Proceedings, 471, 109-114.

[17] Low, B. C., 2001, Coronal mass ejections, magnetic flux ropes, and solar magnetism, Journal of Geophysical Research, 106, Issue A11, 25141-25164.

[18] Gopalswamy, N., Yashiro, S., Akiyama, S., 2007, Geo-effectiveness of Halo CMEs, J. Geophysical Res. 112.

[19] Zhang, J., Dere, K. P., Howard, R. A., & Bothmer, V. 2003, ApJ, 582, 520.

[20] Wang, Y. M., Ye, P. Z., Wang, S., Zhau, G. P., & Wang, J. 2002, J. Geophys. Res., 107, 1340.

[21] Zhao, X.P. and Webb, D.F. 2003. Source regions and storm effectiveness of frontside full halo coronal mass ejections. Journal of Geophysical Research 108.

[22] H. V. Cane, I. G. Richardson, O. C. St. Cyr, 2000, Coronal mass ejections, interplanetary ejecta and geomagnetic storms, Geophysical Research Letters, 27, 21.

[23] Zhang, M.; Low, B. C., 2004, Magnetic Energy Storage in the Two Hydromagnetic Types of Solar Prominences, ApJ, 600, 1043-1051.

TABLE 1. LIST OF HALO CMEs, GEOMAGNETIC STORMS AND CORRESPONDING DIRECTION PARAMETERS

Sl. No	Month	Date	Time (hrs)	CME Width (deg)	Acceln., (m/s^2)	Speed (Km/s)	Date	Time (hrs)	Geo-Mag., Storm (nT)	Transit time (hrs)	Direction parameter (b/a)	Radio burst	X-Ray
1	JAN	02.01.12	15:12:40	360	-8.4	1138	05.01.12	12	-7	75	0.52381	**type IV**	
2		12.01.12	08:24:05	360	-1.1	814	16.01.12	16	-15	104	0.431373		
3		16.01.12	03:12:10	360	10.9	1060	20.01.12	21	-3	114	0.677419		**C6.5**
4		19.01.12	14:36:05	360	54.1	1120	23.01.12	1	-65	109	0.559322		**M3.2**
5		23.01.12	04:00:05	360	28	2175	25.01.12	12	-74	56	0.736842	**type IV**	**M8.7**
6		26.01.12	04:36:05	360	46.2	1194	28.01.12	23	-17	67	0.540541		**C6.4**
7		27.01.12	18:27:52	360	165.9	2507	28.01.12	24	-21	28	0.542857	**type IV**	**X1.7**
8	FEB	02.02.12	14:24:05	360	-8.7	476	06.02.12	21	-17	103	0.354839		
9		09.02.12	21:17:36	360	1.2	659	13.02.12	15	-24	102	0.65625		
10		10.02.12	20:00:05	360	3.8	533	15.02.12	17	-62	123	0.628571		
11		16.02.12	06:36:05	360	1.6	538	19.02.12	5	-54	73	0.5		
12		23.02.12	08:12:06	360	5.5	505	27.02.12	20	-47	108	0.567568		**B5.4**
13		29.02.12	09:12:08	360	-5.4	466	04.03.12	3	-32	126	0.638889		

14	MAR	04.03.12	11:00:07	360	28.3	1306	07.03.12	16	-85	77	0.481481	**type IV**	**M2.0**
15		05,03.12	04:00:05	360	-24.6	1531	09.03.12	9	-143	101	0.491228	**type IV**	**X1.1**
16		07.03.12	00:24:06	360	-88.2	2684	09.03.12	9	-143	57	0.520833	**type II**	**X5.4**
17		09.03.12	04:26:09	360	-13.5	950	12.03.12	17	-51	85	0.825	**type III**	**M6.3**
18		10.03.12	18:12:06	360	24.1	1379	15.03.12	20	-80	122	0.485294	**Type II**	**M8.4**
19		13.03.12	17:36:05	360	45.6	1884	17.03.12	1	-51	112	0.677419	**type II**	**M7.9**
20		18.03.12	00:24:05	360	-8.2	1210	22.03.12	24	-19	120	0.4	**type III**	
21		21.03.12	07:36:05	360	-29.6	1178	24.03.12	8	-15	73	0.433962	**type IV**	
22		24.03.12	00:24:05	360	-46.6	1152	28.03.12	5	-55	101	0.660377	**type III**	
23		26.03.12	23:12:05	360	-32.3	1390	28.03.12	6	-53	65	0.4	**type II**	
24		28.03.12	01:36:07	360	-6.2	1033	02.04.12	20	-29	115	0.368421	**type II**	
25	APRIL	05.04.12	21:25	360	-2.6	828	08.04.12	12	-8	81	0.370968		**C1.5**
26		07.04.12	16:48:05	360	-25.5	765	11.04.12	13	7	99	0.465116	**type**	

												IV	
27		07.04.12	21:15:59	360	3	708	12.04.12	24	-30	123	0.333333		
28		9.04.12	18:24:05	360	-2.8	921	13.04.12	5	-47	109	0.416667	**type IV**	**C3.9**
29		23.04.12	18:24:05	360	-1.1	528	26.04.12	3	-38	87	0.5625		**C2.0**
30		27.04.12	16:24	360	-13.6	681	02.05.12	22	-14	126	0.540541	**type IV**	
31	MAY	12.05.12	00:00:05	360	-6.6	805	16.05.12	24	-38	120	0.425532		**M5.1**
32		17.05.12	01:48:05	360	-51.8	1582	20.05.12	7	-16	91	0.4375	**type IV**	
33		26.05.12	20:57:28	360	-159.2	1966	30.05.12	1	-11	115	0.368421	**type IV**	
34	JUNE	14.06.12	14:12:07	360	-1.2	987	17.06.12	14	-86	75	0.528302		**M1.9**
35		23.06.12	07:24:05	360	-29.1	1263	26.06.12	6	-1	73	0.5		**C3.1**
36		28.06.12	06:24:05	360	-10.4	728	01.07.12	7	-24	73	0.478261		
37	JULY	02.07.12	08:36:04	360	-26.9	1074	06.07.12	22	-23	110	0.372881	**TYPE IV**	
38		04.07.12	17:24:04	360	-37.6	662	07.07.12	14	-4	82	0.646154	**TYPE III**	**M1.8**
39		06.07.12	23:24:06	360	-56.1	1828	09.07.12	13	-69	82	0.362069	**TYPE II**	**X1.1**
40		08.07.12	14:36:05	360	-15.6	796	12.07.12	8	-27	98	0.528571	**TYPE IV**	

41		11.07.12	01:25:27	360	-1.6	379	15.07.12	19	-44	114	0.415385		
42		12.07.12	16:48:05	360	195.6	885	16.07.12	10	-103	102	0.842105	**TYPE III**	**X1.4**
43		19.07.12	05:24:05	360	-8	1631	22.07.12	8	-21	75	0.392157	**TYPE II**	**M7.7**
44		23.07.12	02:36:05	360	-24.6	2003	25.07.12	2	-11	48	0.357143	**TYPE IV**	
45		28.07.12	21:12:08	360	-6.8	420	01.08.12	13	-14	104	0.5		**M6.1**
46		31.07.12	11:24:06	360	-9.3	567	03.08.12	3	-27	80	0.469697		
47	AUG	04.08.12	13:36:23	360	8.9	856	08.08.12	3	-37	106	0.416667		**C3.5**
48		13.08.12	13:25:49	360	-3.5	435	17.08.12	1	-28	100	0.333333		**C2.8**
49		14.08.12	01:25:49	360	16.3	634	19.08.12	13	-34	132	0.5		**C3.5**
50		19.08.12	18:36:05	360	-23	612	22.08.12	6	-20	84	0.64		
51		20.08.12	21:28:11	360	-2.4	521	23.08.12	11	-33	82	0.355932		
52		21.08.12	14:12:06	360	-13.3	575	25.08.12	9	-22	101	0.4375	**TYPE III**	
53		21.08.12	20:24:05	360	-39.9	1024	26.08.12	19	-6	121	0.675676		
54		25.08.12	16:36:05	360	-1.8	636	28.08.12	4	-8	84	0.42		
55		29.08.12	11:48:05	360	-4.9	113	01.09.12	13	-21	82	0.693548		
56		31.08.12	20:00:05	360	2	1442	03.09.12	11	-78	81	0.529412	**TYPE II**	**C8.1**

57	SEP	02.09.12	04:00:06	360	-6.9	538	05.09.12	6	-68	74	0.672727		**C2.9**
58		08.09.12	10:00:06	360	-8.7	734	11.09.12	16	-10	78	0.37037	**TYPE IV**	
59		19.09.12	11:36:06	360	-17.5	616	22.09.12	10	-20	83	0.55	**TYPE II**	
60		19.09.12	13:25:47	360	16.4	525	23.09.12	7	-5	102	0.637931	**TYPE III**	
61		20.09.12	05:48:06	360	-23	633	24.09.12	1	-3	100	0.589744		
62		20.09.12	15:12:10	360	-54.9	1202	24.09.13	2	-1	109	0.377358	**TYPE IV**	
63		21.09.12	06:24:05	360	4.1	639	25.09.12	4	-4	98	0.625		
64		27.09.12	10:12:05	360	-3.6	1319	30.09.12	21	-37	83	0.357143	**TYPE IV**	
65		28.09.12	00:12:05	360	-27.1	947	01.10.12	4	-133	76	0.647059	**TYPE IV**	**C3.7**
66		28.09.12	10:36:05	360	-15.7	768	01.10.12	5	-131	81	0.64		
67		29.09.12	00:12:05	360	-34.4	755	02.10.12	12	-44	84	0.5		